Ultraviolet Radiation Protection by a Beach Umbrella

María P. Utrillas¹, José A. Martínez-Lozano¹ and Manuel Nuñez²

¹Solar Radiation Group, Departamento de Física de la Tierra, Universidad de Valencia, Valencia, Spain ²School of Geography and Environmental Studies, University of Tasmania, Hobart, Tas., Australia

Received 11 June 2009, accepted 25 October 2009, DOI: 10.1111/j.1751-1097.2009.00677.x

ABSTRACT

A beach umbrella intercepts all direct UV irradiance, but only part of the diffuse component. Using a simple sky view factor model, we have determined the fraction of the hemispheric diffuse irradiance that is not intercepted by the umbrella. Assuming a sensor at the surface and close to the center of the umbrella, isotropic diffuse irradiance and for an umbrella of 80 cm radius and 100 cm high, our results show that approximately 34% of the incident horizontal irradiance is not intercepted by the umbrella. These results agree with irradiance measurements conducted with and without the umbrella. The model is next extended to examine receipt of UV radiation by a human figure in a vertical position, either standing or sitting.

INTRODUCTION

UV radiation encompasses wavelengths from 100 to 400 nm of the electromagnetic spectrum. Considered as short wavelength solar radiation, it only comprises 7.2% of the total solar irradiance in the limit of the atmosphere, and unlike the thermal or visible wavelengths, it forms a small fraction of the total solar radiation. There are three bands within the UV spectrum, which are commonly defined by their impact on living organisms: UVC (100–290 nm), UVB (290–320 nm) and UVA (320–400 nm).

The terrestrial atmosphere generally attenuates and modifies solar radiation by scattering and absorption. As a result, solar radiation at the earth's surface is considerably smaller than its extra-terrestrial counterpart. Depletion is quite strong for UV radiation below 290 nm, as a result of column ozone absorption and Rayleigh and Mie scattering. The main factors affecting the magnitude of UV radiation at the earth's surface are solar altitude, the site elevation, reflectivity of the surface, scattering by air molecules and aerosols, column ozone absorption and cloud cover.

Godar (1) has compiled an excellent review of UV radiation and human health, which highlights the following detrimental effects: sunburn (2); photo aging (3,4); eye damage, especially cataracts (5); immune suppression (6,7); DNA damage and mutations (8); and skin cancers (9–11). UV exposure can also affect human health in beneficial ways. It is used to treat skin and other diseases, is necessary for vitamin D3 formation (12),

*Corresponding author email: jose.a.martinez@uv.es (Jose A. Martínez-Lozano) © 2010 The Authors. Journal Compilation. The American Society of Photobiology 0031-8655/10

possibly lowers hypertension (13,14) and reduces the occurrence of some internal cancers such as prostate cancer (15).

The public considers a tan to be the major benefit of UV exposure but some scientists view a tan, along with sunburn, as a warning that too much UV exposure and subsequent damage has occurred to the skin. UVR exposure can cause skin cancer (16).

The UVB wavelengths have the most carcinogenic potential according to the photocarcinogenesis action spectrum (17,18). Nonmelanoma skin cancers (NMSC), basal cell carcinomas (BCC) and squamous cell carcinomas (SCC) are almost exclusively caused by cumulative UV exposure, while cutaneous malignant melanoma (CMM) has one or more additional contributing factors: sunburns, number of nevi, genetic background, chemical exposure or other factors. In 2002 there were over one million new cases of nonmelanoma and melanoma skin cancers in the United States (19). CMM has been increasing in fair-skinned individuals at a logarithmic rate over the past seven decades.

Increase in leisure time and a better quality of life has increased this exposure to the sun, often to quite high levels of UV radiation. Typical population exposure examples are 220 SEDs year⁻¹ (standard erythema doses per year) for women and 280 SEDs year⁻¹ for men (20,21) and annual doses of 313 and 231 SEDs for men and women in Spain (22).

The effects of UV radiation on human skin centers on the concept of erythemal UV radiation (UVER), which is determined by convolving spectral solar radiation incident at the earth's surface with the eythema action spectrum. This action spectrum, a response of human skin to incident UV radiation, has a maximum from 200 to 297 nm (23) and decreases at longer wavelengths. In 1987 the Commission Internationale d'Eclairage adopted the "Standard Erythema Curve" (24) which is presently used to estimate UVER.

Mechanisms of photo-protection in response to UVER may be classified into three groups: physical barriers, and chemical and biological agents. We can view any reflecting or absorbing material as being a physical barrier, such as the earth's atmosphere in the case of incoming solar radiation, which constitutes its first filter. The unpolluted atmosphere, under summer, cloudless noon-time conditions, will reduce erythemal radiation by a factor of 20, and by a factor of 30 in polluted conditions, compared to the extra-terrestrial solar UV spectrum. Other natural barriers include buildings and trees (25–29). Garments are also good physical barriers, and provide the main protection for individuals exposed to the sun. Their effectiveness depends on the texture and colors, *etc.* although it

is usually necessary to utilize additional protection. The simplest one is to reduce the number of hours exposed to the sun corresponding to times of high solar elevation, and to use protective clothing, wide-brimmed hats with at least a 7 cm brim and UV-protective sunglasses.

A commonly used physical barrier employed in outdoor activities is the beach umbrella. They come in many different materials and sizes. In this manuscript we present results on the UV transmission of an umbrella of canvas, painted white and blue, and radius and height of 0.8 and 1.5 m, respectively. Our procedure is to develop a simple geometrical model which estimates the UV radiation received from a sky that is partially obstructed. Model predictions are then compared with measurements performed with the above typical umbrella.

It is evident that the umbrella on its own does not offer total sun protection, but may be viewed as an additional physical barrier. Additional protection from sunscreens is usually recommended, these varying according to skin type, which in Spain is Type 2–3.

MATERIALS AND METHODS

A sky view factor model. In applying these concepts to a beach umbrella, we assume first that all direct radiation is absorbed by the umbrella (it depends on the transmissivity of the material which in our case is 4%. See Results section), so UV radiation incident on the individual is only by diffuse sky radiation. The diffuse irradiance received by a detector at the earth's surface from a partially obstructed sky may be examined by constructing an imaginary hemisphere around the detector. Each sky or obstructing element δA will trace a ray between itself and the sensor, which will intersect with the hemisphere at solid angle $\delta\omega$. The total irradiance received by the detector is

$$I = \int_{\omega=0}^{2\pi} L \cos(i)\delta\omega \tag{1}$$

where i is the incidence angle, and the integration is performed over the entire hemisphere, subtending a solid angle of 2π . Let us now partition the integration into elements exposed to the sky and obstructing elements and assume that the radiance from each of these two elements, sky and obstruction, is isotropic. Equation (1) may then be written as:

$$I = L_{\rm SKY} \int^{\omega_{\rm SK}} \cos(i) \delta\omega \, + \, L_{\rm OBS} \int^{\omega_{\rm OBS}} \cos(i) \delta\omega \eqno(2)$$

and the integration is performed over all solid angles containing sky $(\omega_{\rm SKY})$ and obstruction $(\omega_{\rm OBS})$ elements. Noting also that

$$\int_{\omega=0}^{2\pi}\cos(i)\delta\omega=\pi,$$

we can re-write Eq. (2) as:

$$I = \pi L_{\text{SKY}}(\text{SVF}) + \pi L_{\text{OBS}}(1 - \text{SVF})$$

$$\text{SVF} = \frac{\int_{0}^{\omega_{\text{SKY}}} \cos(i)\delta\omega}{\pi}$$
(3)

where SVF is popularly defined as the "Sky View Factor", varying between 1 for an uninterrupted sky view and 0 for a totally obstructed sky. Estimating SVF is a geometrical problem and in the Appendix we describe how SVF is calculated for a horizontal sensor located at the surface and vertically underneath the center of an umbrella, therefore mimicking the energy received by a human body stretched under the umbrella.

Experimental measurements. Erythema irradiance was measured using YES radiometers. The YES-UVB-1, whose spectral interval is from 280 to 400 nm, consists of a phosphor that converts UV into visible light which is precisely measured using a solid state photodiode. The direct and diffuse incident solar radiation is transmitted through the YES-UVB-1 quartz dome. The visible light, except for a small fraction in the red part of the spectrum, is absorbed by black glass which transmits only the UV component. The light transmitted by the filter falls on the phosphor which absorbs the UVB component and reemits visible light by fluorescence, mostly at green wavelengths. The fluorescent light from the phosphor passes through a green glass filter to remove the red light that had passed through the first "black" filter. The intensity of the remaining fluorescent light is measured by a solid state diode (GaAsP), which has a maximum sensitivity in the green spectrum and is not sensitive to red light. All the optical components, the detector and filters are stabilized at a temperature of $(45 \pm 1)^{\circ}$ C for an ambient temperature between -40 and +40°C.

To measure diffuse irradiance we built a semicircular shadowband with its plane perpendicular to a supporting shaft which is facing true north and is of an inclination equal to the local latitude. The radiometer, placed on a platform at the center of the shadowband, only senses diffuse radiation as the shadowband blocks all direct sunlight. This low-cost design has been built following Horowitz (30) and its main components may be seen in Fig. 1. The radiometer data must be corrected for the fraction of the sky that is blocked by the shadowband. There are various methods to perform this correction and based on previous work (31), we have opted for using the modified Batlles model (32) as it performed best.

To determine the transmissivity of the umbrella, we measured UVER with the umbrella touching the sensor followed by a second measurement without the umbrella. Measurements were made in December under totally cloudless skies with results shown in Fig. 2. As may be seen, the umbrella has an average transmissivity of 0.04 or 4%. Grifoni et al. (33) employed a similar method to obtain a transmissivity value of 3.9%. Estimates by Turnbull and Parisi (25) using spectral methods are substantially lower (0.9%), and it is likely that these differences are due to different colors and textures that were used for the umbrellas.

RESULTS

UVER received by a horizontal sensor under the umbrella

From Eq. (3) and the definition of SVF in the Appendix, we can write the irradiance for a horizontal sensor under the umbrella as:



Figure 1. Experimental arrangement used to measure diffuse UVER.

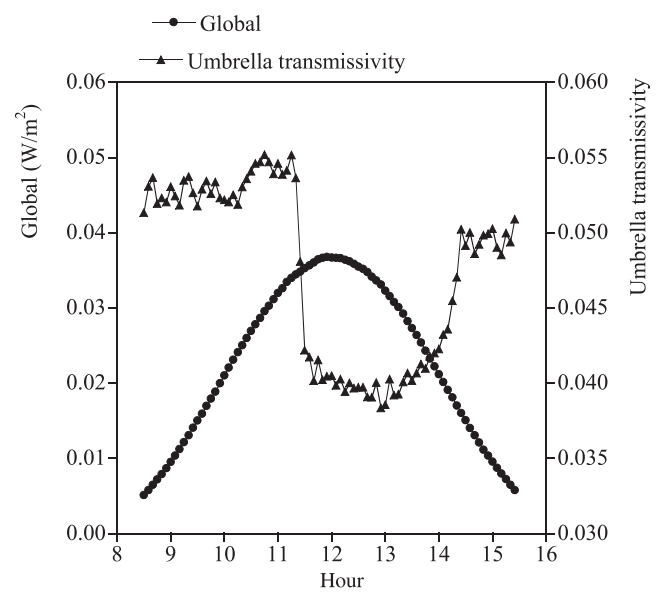


Figure 2. Transmissivity of the umbrella texture. Measurements were taken on a cloudless day, 18 December 2008. Measurements taken during the hours of 11.00 and 14.00 are considered as representative of texture transmission as they were not corrupted by direct irradiance.

$$I_{Hz} = \pi L_{SKY}(SVF) + \pi L_{OBS}(1 - SVF)$$

= $\pi L_{SKY}(1 - \sin^2 \theta) + \pi L_{OBS}(\sin^2 \theta)$ (4)

The radiance from the sky and umbrella obstruction may be readily obtained from the measurements assuming isotropy:

$$L_{\rm SKY} = \frac{I_{\rm DF}}{\pi}$$

$$L_{\rm OBS} = I_{\rm BHZ} \times 0.04 + \frac{I_{\rm DF} \times 0.04}{\pi}$$
(5)

where $I_{\rm DF}$ and $I_{\rm BHz}$ are diffuse and direct horizontal irradiance, respectively.

We consider the umbrella to have a height of 100 cm and a radius of 80 cm. The horizontal sensor, located at ground level, subtends an angle θ between its vertical and the umbrella edge. Applying the value of 38.6° for θ and substituting in Eq. (4), we obtain the total horizontal irradiance at ground level and in the umbrella center. Figure 3 shows measured irradiance above the umbrella and modeled irradiance underneath for one cloudless day, 26 July, between the hours of 10.5 and 13.5 GMT. A mean transmission of 34% is obtained over the period of measurement.

These results were validated during an experiment performed in July 2008. Two YES UB-1 radiometers were deployed on the roof of Block C Faculty of Physics, approximately 3 m apart. One instrument was exposed to the full sky, and the second was placed in a horizontal position, at ground level and directly underneath the umbrella center, thus mimicking the UV load received by a human being lying down. Measurements were conducted between the hours of 10.0 and 14.0 GMT.

Figure 3 presents the irradiance above the umbrella and the modeled and measured irradiance beneath as described in the above paragraph. Both modeled and measured irradiance

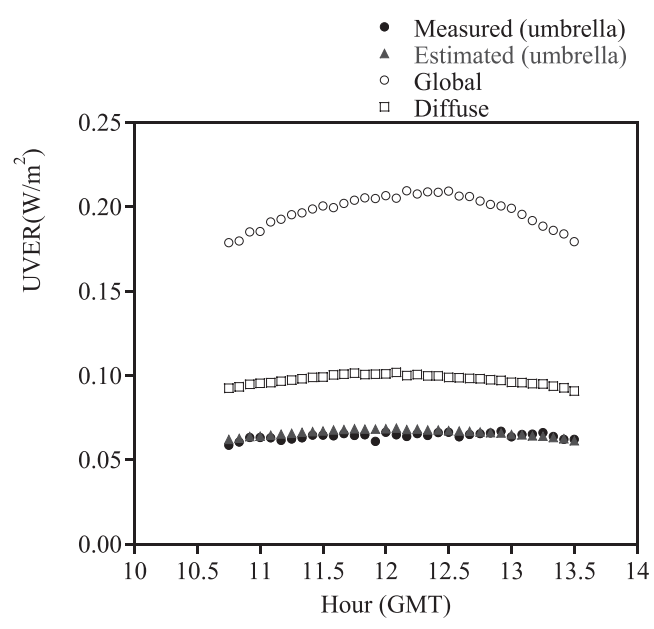


Figure 3. Global and diffuse irradiance measured above the umbrella and measured and modeled irradiance below the umbrella. Measurements were taken on 26 July 2008.

agree closely, with mean values of 0.066 and 0.064 W m⁻², describing a relative error of 2.9%. The data may also be presented as a fraction of the irradiance above, as shown in Fig. 4. Both theory and measurements provide a mean estimate of 33% for the transmission of the UV irradiance above the umbrella.

UVER received by a vertical sensor under the umbrella

It may also be of interest to estimate the irradiance load on a vertical surface, an approximation to that received by a standing human being. The receiving surface and therefore the view factor hemisphere rests along the torso (Fig. 5a).

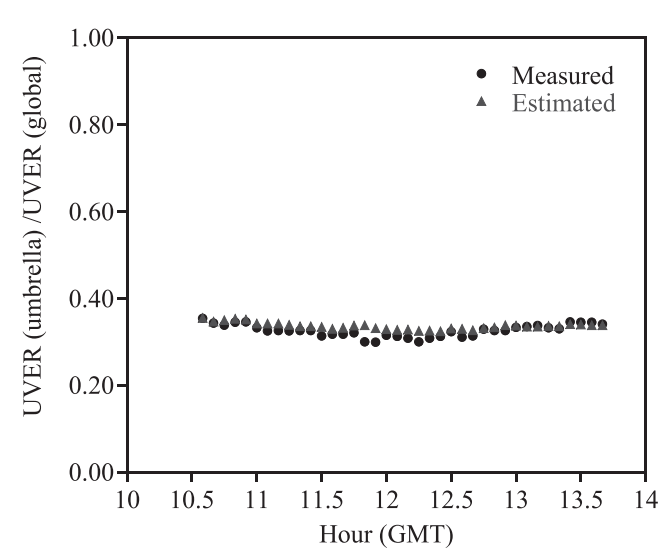
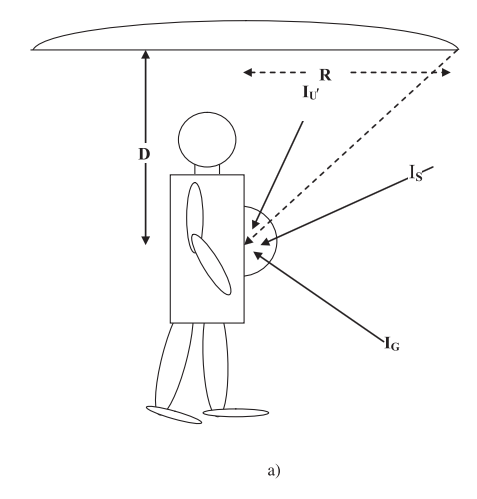


Figure 4. As in Fig. 3, but showing measured and modeled irradiance below the beach umbrella expressed as a fraction of incident irradiance.



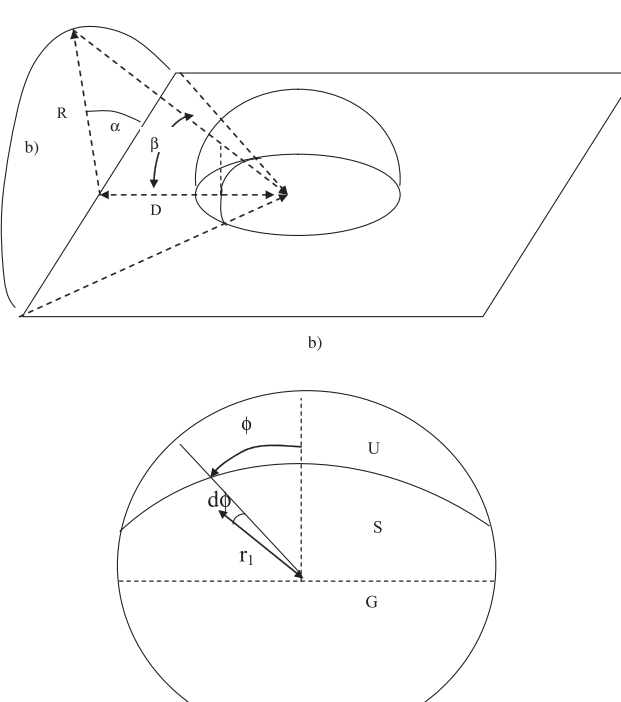


Figure 5. (a) Schematic showing the projection of a beach umbrella on a vertical surface viewed as the load received by a human figure on the torso. (b) Radiance from the umbrella projects onto a crescent-shaped figure in the plane of the receiving surface. (c) Horizontal projection showing the contribution of the various surfaces to the view factors. The crescent-shaped area denoted by U represents the contribution from the umbrella, while S and G represent contributions from the sky and ground, respectively.

Radiance load on the torso comes from the umbrella $(I_{\rm U})$, the sky (I_S) and the ground (I_G) . Critical dimensions are distance from the receiving surface to the umbrella edge (D) and radius of the umbrella (R). For clarity we tilt the axes and view the umbrella configuration as standing vertical and the receiving surface on the horizontal (Fig. 5b).

The radiance from the umbrella is projected onto the plane of the sensor where it describes a crescent-shaped figure. This crescent-shaped area defines the contribution of the umbrella

to the total view factor. Examining the umbrella in more detail, we can define three contributions to the view factor, the sky, the umbrella and the surface as in Fig. 5c. The area U may be explicitly written as:

$$U = 2 \int_{\varphi=0}^{\varphi=\tan^{-1}(R/D)} (1 - r_1) d\varphi = 2 \int_{\varphi=0}^{\varphi=\tan^{-1}(R/D)} (1 - \cos \beta) d\varphi$$

$$= 2 \int_{\varphi=0}^{\varphi=\tan^{-1}(R/D)} \left(1 - \cos \left[\tan^{-1} \left\{ \frac{R \sin \alpha}{[D^2 + R^2 \cos^2 \alpha]^{1/2}} \right\} \right] \right) d\varphi$$
and $\tan \varphi = \frac{R \cos \alpha}{D}$ (6)

Keeping in mind that the area of a circle of unit radius is π , we can write the irradiance on a vertical surface as:

$$I_{90^{\circ}} = (\text{UVF})I_{\text{IJ}} + (\text{SVF})I_{\text{S}} + (\text{GVF})I_{\text{G}}$$
 (7)

where UVF is the umbrella view factor, SVF is the sky view factor and GVF is the ground view factor.

Equation (6) may be solved numerically as a function of distance of the receiving surface from the umbrella edge (D)and the umbrella radius (R). Table 1 shows the sky and umbrella view factors for different combinations of R and D.

The total irradiance load in the vertical, estimated using Eqs. (6) and (7), is shown in Fig. 6 for one cloudless day, 6 May. Measured values above the umbrella are contrasted against the much lower irradiance load in the vertical. The percentage transmission values indicate a relatively constant transmission of around 17% during the period of measurement. This figure is considerably lower than the equivalent figure of 33% obtained for a horizontal sensor. Clearly the low ground albedo estimate (~4.5%) and the high ground view factor of 0.5 combine to lower the overall UV load.

In the real practical case, human beings are not always underneath the umbrella center, but at varying distances from it. Mathematical modeling of these special configurations may be tedious and complex and may not approach reality as there may be many other sky obstructions which are hard to quantify. In this case SVF photographs (or fish-eye lens photographs) are one practical option. The advantage is that they capture the entire hemispherical view including all obstructions, and in addition the camera sensor may be placed in any position and angle. In this study we follow the method of Steyn (34), which processes prints from photographic images to obtain SVF. The essential procedure consists in estimating relative areas from the print using manual integration while applying an angular correction that depends on the angular distance of any pixel from the image nadir.

To test the technique, the radiometer sensor was placed in the vertical, at 40 cm from the umbrella center and at 85 cm from the surface (45 cm from umbrella edge). Fish-eye lens photographs were taken at the position corresponding to the sensor facing south and north, respectively. Results are shown in Table 2 for vertical planes facing North and South, respectively. These images provide sky (SVF), Umbrella (UVF) and ground (GVF) view factor used in Eq. (7) for estimating irradiance loads.

In Fig. 7a,b we present measured horizontal irradiances above and vertical irradiance underneath the umbrella, along

Table 1. Sky view factor (SVF) and umbrella view factor (UVF) for different combinations of umbrella radius (R) and vertical distance (D) from the umbrella edge.

R (m)	D (m)	UVF	SVF 0.12475	
0.5	0.1	0.37525		
0.5	0.45	0.10822	0.39178	
0.5	0.75	0.04016	0.45984	
0.5	1	0.02021	0.47979	
0.5	1.5	0.00691	0.49309	
0.5	2	0.00308	0.49692	
0.6	0.1	0.39508	0.10492	
0.6	0.45	0.14206	0.35794	
0.6	0.75	0.05936	0.44064	
0.6	1	0.03151	0.46849	
0.6	1.5	0.01133	0.48867	
0.6	2	0.00515	0.49485	
0.7	0.1	0.40952	0.09048	
0.7	0.45	0.17297	0.32703	
0.7	0.75	0.08007	0.41993	
0.7	1	0.04475	0.45525	
0.7	1.5	0.01696	0.48304	
0.7	2	0.0079	0.4921	
0.75	0.1	0.41535	0.08465	
0.75	0.45	0.18714	0.31286	
0.75	0.75	0.09064	0.40936	
0.75	1	0.05192	0.44808	
0.75	1.5	0.02021	0.47979	
0.75	2	0.00953	0.49047	
0.8	0.1	0.42047	0.07953	
0.8	0.45	0.20046	0.29954	
0.8	0.75	0.10121	0.39879	
0.8	1	0.05936	0.44064	
0.8	1.5	0.02373	0.47627	
0.8	2	0.01133	0.48867	
1	0.1	0.43597	0.06403	
1	0.45	0.24577	0.25423	
1	0.75	0.14206	0.35794	
1	1	0.09064	0.40936	
1	1.5	0.04016	0.45984	
1	2	0.02021	0.47979	

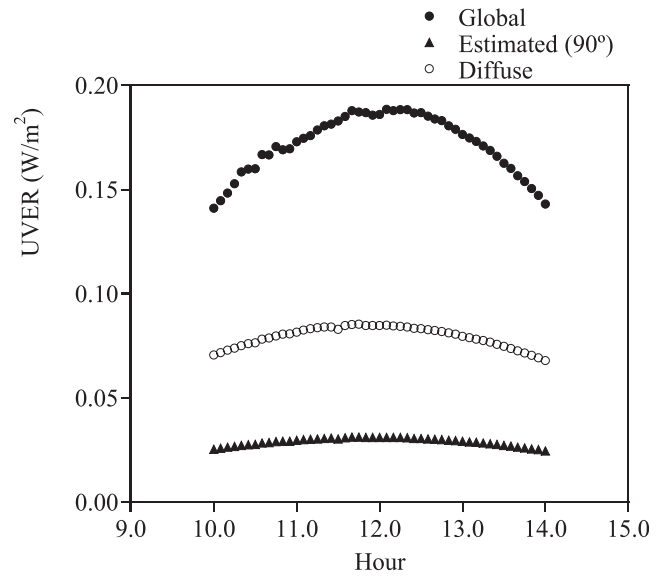


Figure 6. Measured global irradiance above the beach umbrella and modeled for a vertical sensor located underneath the center of the beach umbrella and at a vertical distance of 45 cm from the umbrella edge. Measurements were taken on 6 May 2009.

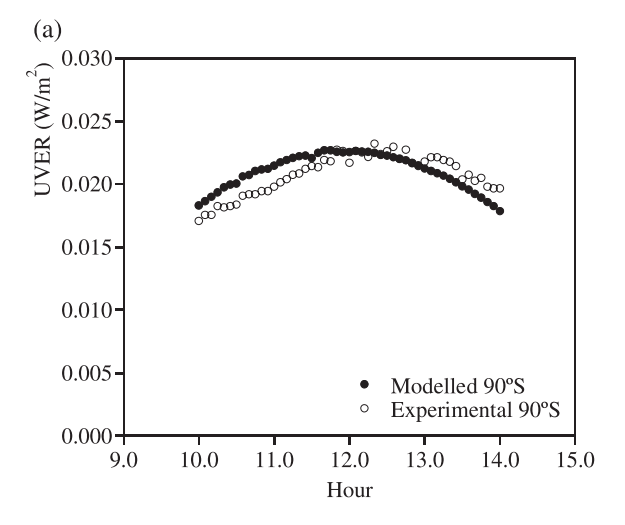
with modeled irradiance using the photographs for 6 May 2009. Measured and modeled irradiances show good agreement for both orientations throughout the day, and agree closely at noon. Both orientation data sets have a root mean square error of 6% with respect to the measured data, and mean bias errors (model - measured) of 4.0 and 1.5% for the north and south orientations, respectively.

Application to other environments

The method described in this study may be applied to model irradiance loads in other complex environments. Furthermore, it is expected that there will be substantial differences in the

Table 2. View factors from fish-eye lens photographs.

South-facing		North-facing		
Sky view factor	0.19	Sky view factor	0.28	
Umbrella view factor	0.30	Umbrella view factor	0.01	
Ground view factor	0.50	Ground view factor	0.50	
Sky obstructions	0.01	Sky obstructions	0.11	
Total	1.00	Total	1.00	



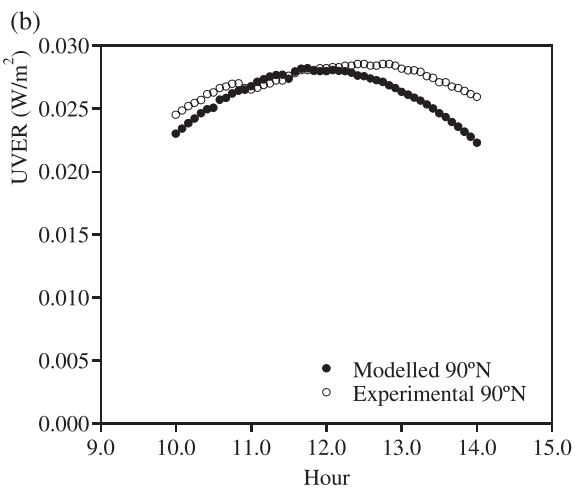


Figure 7. Comparison of measured vs modeled vertical irradiance using sky view factors from fish-eye lens photographs. (a) Facing north. (b) Facing south.

Table 3. UV load ratios for two umbrella configurations and six surface types. The umbrella has a radius of 0.8 m but is positioned at two different heights above the surface—2.0 m and 1.5 m. Ratios are expressed as irradiance received by the face as a fraction of global horizontal irradiance in the open (*G*).

Umbrella height (m)	Grass	Water	Concrete	Sand	Saltpan	Snow
2.0 (S)	0.23 (5)	0.24 (5)	0.28 (4)	0.29 (4)	0.62 (1)	0.77 (1)
2.0 (L)	0.42(3)	0.42 (3)	0.44(3)	0.44(3)	0.54(2)	0.58(2)
1.5 (S)	0.17 (6)	0.18 (6)	0.22 (5)	0.23 (5)	0.55(2)	0.69(1)
1.5 (L)	0.39 (3)	0.39 (3)	0.40(3)	0.40 (3)	0.49 (2)	0.53(2)
$G(\hat{W}m^{-2})$	313.6 (153)	316.0 (154.9)	324.6 (163.5)	325.9 (164.8)	419.4 (258.3)	480.3 (319.2)
Albedo	0.02	0.04	0.11	0.12	0.69	0.94

Numbers refer to diffuse irradiance. Symbols S and L refer to sitting and lying, respectively. In parenthesis, the approximate SPF corresponding to every case is presented. See text for further details.

overall load as a function of the albedo properties of the surface. Our measured roof albedo was 4.5%, implying a very low radiance contribution from the surface, and a substantial reduction in the overall irradiance load for the vertical surface.

As an example of how the technique may be applied, we examined UVER loads with two umbrella configurations for six different surfaces. Average values were taken for grass, water and sand (35–38), concrete (39) and two high albedo surfaces, salt flats (40) and fresh snow (41).

Two umbrella configurations were chosen, one configuration had the umbrella edge 2 m above the surface, the second configuration had the umbrella edge lower, at 1.5 vertical meters above the surface. For each configuration we estimate the UV load on the face for one person lying down under the umbrella center and that received while sitting also under the center. In the sitting position we have taken the vertical distance from the face to the umbrella edge as 1 and 1.5 m from the lower and taller umbrella, respectively. Global and diffuse irradiance in the open was modeled using LibRadtran, solar zenith angle of 20°, for a mid-latitude summer atmosphere, total ozone column of 250 DU and 30 km horizontal visibility. Different albedos were used, which provided incoming global and diffuse irradiance.

Table 3 shows the results. Statistics show a dependence on surface albedo. At the lower albedo range, the individual lying down receives a higher load compared to the person sitting. This is due to the fact that when sitting, the sky portion seen is lower, and as a result diffuse sky radiation is also lower but ground-reflected diffuse radiation is higher. By contrast, when lying there is a larger portion of sky radiation that is received. In the case of grass and with a 2 m high umbrella, this figure is 42% of the open exposure. Even lowering the umbrella to 1.5 m only lowers the exposure by a few percent, to 39% of the open. By contrast the person sitting will only receive 23 and 17% of the open exposure depending on umbrella height. This figure remains very similar for the low surface albedos considered here (grass, water, sand, concrete). However, for high albedos, the reverse occurs. Now the person sitting receives the highest exposure as a result of the high surface albedo (for example 77% for a person sitting in snow under a 1.5 m high umbrella).

The umbrella eliminates 67% of the UV radiation incident on a horizontal sensor, and nearly 83% when the sensor is positioned vertically. As a result we can assign solar protection factors (SPFs) of 3–4 and 7–8 for the first and second position, respectively. These SPF estimates, representative of a small umbrella, will increase with umbrella diameter.

CONCLUSIONS

We have modeled and measured typical irradiances received under a beach umbrella both in the horizontal and vertical plane. Absorption of UV radiation by the material of the umbrella is high, with only 5% of the UVER being transmitted. Nevertheless the irradiance that reaches the sensor at the base is 34% of the irradiance in the open. These results point to the importance of diffuse UV radiation in the total UV load experienced by human beings in beach environments. The beach umbrella effectively blocks direct radiation, but diffuse radiation, approximating 60% of the global radiation in the UVER (32), still reaches the sensor from the unimpeded sky.

We have estimated the received irradiance using a simple sky obstruction geometrical model. In the case of horizontal irradiance the model agreed well with measured data, with a relative error of only 3%. This error could arise from assumptions regarding isotropy of the diffuse radiation. Our estimates of sky radiance are based on pyranometer measurements of diffuse irradiance from the entire hemisphere. Sky radiances near the solar zenith are underestimated, while radiances near the horizon, as in our case, are probably overestimated. On the other hand, the likely presence of sky obstructions near the horizon would counter this effect.

In some cases human beings are not always lying under the umbrella, but may be sitting or standing. To model this process we have considered the irradiance received on a vertical surface at the ground and near the umbrella pole, and at approximately one half the length of the radius away from it and 85 cm above the surface. In both cases relevant view factors have been obtained for the sky, ground and umbrella.

Results show that approximately 17% of the unimpeded irradiance reaches the vertical sensor, with good agreement between measurements and theory. For the sensors further apart from the center, the north-facing sensor receives 16% of the uninterrupted irradiance, while the south-facing slope receives 12%. RMS errors between model and measurements are satisfactory, around 6%.

Future developments could consider the more complex case typical of crowded beaches when neighboring umbrellas impinge on the sky field of view of the sensing element considered in this study. In general terms a greater degree of protection would occur, with the actual amount depending on the density and location of the closest umbrellas.

We conclude by noting that human beings inhabit complex physical environments where the radiation field may be blocked, reflected or depleted several times before reaching the human body. Assessing these UV loads is difficult but necessary to understand the epidemiology of some skin cancers. The method provided here can help not only to determine these UV loads but can also illuminate how the physical characteristics of the environment contribute to these loads, mainly through the interaction of view factors, albedos and incoming surface irradiance.

Acknowledgements-This work was funded by the Ministerio de Ciencia e Innovación, Spain, through the Project CGL2007-60648. M. Nuñez staved in Valencia thanks to the Convocatòria d'estades temporals d'investigadors convidats de la Universitat de València.

APPENDIX

View factor concepts

In this section we review the concept of sky view factor (SVF) as impacting on a radiometer sensor at the earth's surface, which is initially considered to be horizontal. The sensor is considered to be at the center of a sky hemisphere as shown in

Any radiance from the sky L (W m⁻² ster⁻¹) is characterized by an element of solid angle $\delta\omega$ equal to $\sin\theta d\theta d\phi$. Assuming a perfect cosine receptor, the energy recorded by the sensor is $L\cos\theta\sin\theta d\phi$. For isotropic radiation, a simple expression I may be derived for the total flux recorded by the sensor (34,42):

$$I = \int_{\varphi=0}^{\varphi=2\pi} \int_{\theta=0}^{\theta=\pi/2} L \sin \theta \cos \theta \, \mathrm{d}\theta \, \mathrm{d}\phi = \pi L$$

For an arbitrary element δA , the contribution is $L\delta A'\cos\theta'$, where $\delta A'$ is the projection of δA on the surface of the sphere. However, the quantity $\delta A' \cos \theta'$ is also the projection of $\delta A'$ on the horizontal surface, $\delta A''$ (see Fig. 1). The SVF, or the fraction of the sky that contributes to the total irradiance, may then be written as:

$$SVF = \frac{L \int \delta A''}{L\pi R^2}$$

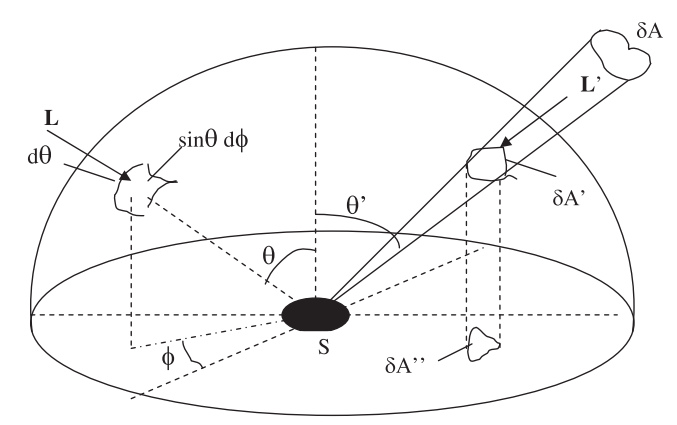


Figure 8. Radiance L from the sky hemisphere incident on a sensor S. L is characterized by an increment of solid angle $\delta\omega$ equal to $\sin \theta d\phi$. Radiation from an arbitrary element of area δA intersects the hemisphere at $\delta A'$.

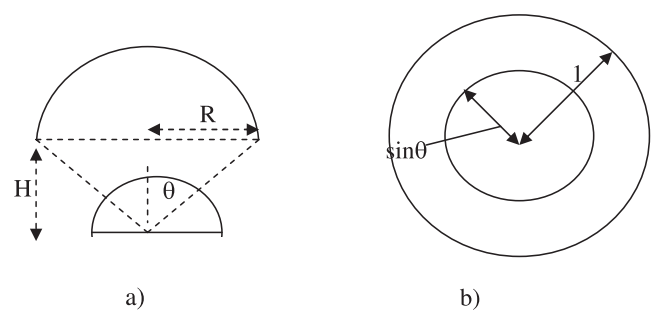


Figure 9. (a) Vertical cross-section showing a unit hemisphere at the surface and the intersection of the umbrella edge with the hemisphere. (b) Horizontal projection for the unit hemisphere. The area of the hemisphere projection that is shaded by the umbrella is denoted as $\pi \sin \theta^2$.

and the $L\pi R^2$ term represents the contribution from the entire sky. Therefore, assuming isotropy and unit radius the irradiance contribution from any surface is $\pi L(SVF)$.

The same concept may be applied for a beach umbrella (Fig. 9a), with the sensor being at the surface, and the critical dimensions being the height of the umbrella edge (H) and its radius R. The angle of intersection of the umbrella edge with the sky hemisphere is given as $\theta = \tan^{-1}(R/H)$. Figure 9b shows the horizontal projection for this configuration. The inner circle with radius $\sin\theta$ represents the projection for the shaded portion of the sphere, the larger circle is the entire projection. Therefore the view factors are $\pi \sin^2 \theta$ and $(\pi \pi \sin^2 \theta$) for the umbrella sky, respectively. Assuming isotropy in the radiance field for both sources, the total irradiance R may be described as:

$$I = (\pi \sin^2 \theta) L_{\rm U} + (\pi - \pi \sin^2 \theta) L_{\rm S}$$

REFERENCES

- 1. Godar, D. E. (2005) UV doses worldwide. Photochem. Photobiol. 81, 736-749.
- 2. Daniels, F. J., Jr, C. van der Leun and B. E. Johnson (1968) Sunburn. Sci. Am. J, 219, 38-46.
- Yaar, M. and B. A. Gilchrest (1998) Aging and photoaging: Postulated mechanisms and effectors. J. Invest. Dermatol. Symp. Proc. 3, 47-51
- 4. Godar, D. E., M. L. Swicord and L. H. Kligman (1995) Photoaging. In Environmental UV Radiation and Health Effects (Edited by H.-J. Schopka and M. Steinmetz), pp. 123-131. BfS-ISH-Berichte, Munich-Neuherberg.
- 5. Sliney, D. H. (1994) Epidemiological studies of sunlight and cataract: The critical factor of ultraviolet exposure geometry. Ophthalmic Epidemiol. 1, 107-119.
- Vink, A. A., D. B. Yarosh and M. L. Kripke (1996) Chromophore for UV-induced immunosuppression: DNA. Photochem. Photobiol. 63, 383-386.
- 7. Nishigori, C., D. B. Yarosh, C. Donawho and M. L. Kripke (1996) The immune system in ultraviolet carcinogenesis. J. Invest. Dermatol. Symp. Proc. 1, 143-146.
- Wikonkal, N. M. and D. E. Brash (1999) Ultraviolet radiation induced signature mutations in photocarcinogenesis. J. Invest. Dermatol. Symp. Proc. 4, 6-10.
- Urbach, F. (1991) Incidence of nonmelanoma skin cancer. Dermatol. Clin. 9, 751-755.
- 10. Elwood, J. M. and J. Jopson (1997) Melanoma and sun exposure: An overview of published studies. Int. J. Cancer 73, 198-203.

- 11. Lev. R. D. and V. E. Reeves (1998) Chemoprevention of ultraviolet radiation-induced skin cancer. Environ. Health Perspect. 105, 981-984.
- 12. Holick, M. F., J. A. MacLaughlin, M. B. Clark, S. A. Holick, J. T. Potts Jr, R. R. Anderson, I. H. Blank, J. A. Parrish and P. Elias (1980) Photosynthesis of pre-vitamin D3 in human skin and the physiological consequences. Science 210, 203-205.
- 13. Rostand, S. G. (1997) Ultraviolet light may contribute to geographic and racial blood pressure differences. Hypertension 30, 150-156.
- 14. Weber, K. T., E. W. Rosenberg and R. M. Sayre (2004) Suberythemal ultraviolet exposure and reduction in blood pressure. Am. J. Med. 117, 281–292.
- 15. Luscombe, C. J., A. A. Fryer, M. E. French, S. Liu, M. F. Saxby, P. W. Jones and R. C. Strange (2001) Exposure to ultraviolet radiation: Association with susceptibility and age at presentation with prostate cancer. Lancet 358, 641-642.
- 16. Altmeyer, P., K. Hoffman and M. Stucker (eds) (1997) Skin Cancer and UV Radiation. Springer-Verlag, Berlin.
- 17. de Gruijl, F. R., H. J. Sterenborg, P. D. Forbes, R. E. Davies, C. Cole, G. Kelfkens, H. van Weelden, H. Slaper and J. C. van der Leun (1993) Wavelength dependence of skin cancer induction by ultraviolet irradiation of albino hairless mice. Cancer Res. 53, 53-
- 18. de Gruijl, F. R. and J. C. van der Leun (1994) Estimate of the wavelength dependency of ultraviolet carcinogenesis in humans and its relevance to the risk assessment of stratospheric ozone depletion. Health Phys. 67, 319-325.
- 19. Goldman, E. I. (2002) Skin cancer prevention messages target teens: Peer pressure, vanity often trump prudence. Skin and Allergy News 33(6), 1-4.
- 20. Godar, D. E., S. P. Vegrati, J. Shreffler and D. H. Sliney (2001) UV doses of Americans. Photochem. Photobiol. 73, 621-629.
- 21. Godar, D. E., F. Urbach, F. P. Gasparro and J. C. van der Leun (2003) UV doses on young adults. Photochem. Photobiol. 77, 453-
- 22. Gurrea, G. and J. Canada (2007) Study of UV radiation dose received by the Spanish population. Photochem. Photobiol. 83, 1364-1370
- 23. Diffey, B. L. (1982) The consistency of studies of ultraviolet erythema in normal human skin, Phys. Med. Biol. 27, 715-720.
- 24. McKinlay, A. F. and B. L. Diffey (1987) A reference spectrum for ultraviolet induced erythema in human skin. CIE J. 6, 17-22.
- 25. Turnbull, D. J. and A. V. Parisi (2003) Spectral UV in public shade settings. J. Photochem. Photobiol. B, Biol. 69, 13-19.
- 26. Turnbull, D. J. and A. V. Parisi (2005) Increasing the ultraviolet protection provided by shade structures. J. Photochem. Photobiol. B, Biol. 78, 61–67.

- 27. Turnbull, D. J. and A. V. Parisi (2004) Annual variation of the angular distribution of the UV beneath public shade structures. J. Photochem. Photobiol. B, Biol. 76, 41-47.
- 28. Collins, D. C. A., R. A. Kearns and H. Mitchell (2006) "An integral part of the children's education": Placing sun protection in Auckland primary schools. Health & Place 12, 436-448.
- 29. Heisler, G. M., R. H. Grant and W. Gao (2003) Individual and scattered-tree influences on ultraviolet irradiance. Agric. For. Meteorol. 120, 113-126.
- 30. Horowitz, J. L. (1969) An easily constructed shadow-band for separating direct and diffuse solar radiation. Solar Energy 12, 543-545.
- 31. Utrillas, M. P., A. Esteve, M. J. Marin, F. Tena, J. Cañada and J. A. Martinez-Lozano (2007) Diffuse UVER radiation experimental values. J. Geophys. Res. 112, D24207. DOI: 10.1029/ 2007JD008846
- Batlles, F. J., F. J. Olmo and L. Alados-Arboledas (1995) On shadowband correction methods for diffuse irradiance measurements. Solar Energy 54, 105-114.
- 33. Grifoni, D., G. Carreras, F. Sabatini and G. Zipoli (2005) UV hazard on a summer's day under Mediterranean conditions and the protective role of a beach umbrella. Int. J. Biometeorol. 50, 75-82.
- 34. Steyn, D. G. (1980) The calculation of view factors from fish-eye lens photographs. Atmos. Ocean 18, 254-258.
- 35. Chadysiene, R. and A. Girgzdys (2008) Ultraviolet radiation albedo of natural surfaces. J. Env. Eng. Landscape Mgt. 16, 1683-
- 36. De Paula, C. and J. C. Ceballos (2008) UVB surface albedo measurements using biometers. Rev. Brasileira de Geofis. 26, 411-
- 37. Parisi, A. V., J. Sabburg, M. G. Kimlin and N. Downs (2003) Measured and modelled contributions by the albedo of surfaces in an urban environment. Theor. Appl. Climatol. 76, 181-
- 38. McKenzie, R. L., L. Kotkamp and W. Ireland (1996) Upwelling UV spectral irradiance and surface albedo measurements at Lauder, New Zealand. Geophys. Res. Lett. 23, 1757-1760.
- 39. Castro, T., L. Morales, R. Longoria and L. G. Ruiz Suarez (2001) Surface albedo measurements in Mexico city metropolitan area. Atmosfera 14, 69-74.
- 40. Andrade, M. and F. Zaratti (2007) Medidas de albedo en Solar de Uyeni. Rev. Boliviana Fis. 13, 11-17.
- Blumthaler, M. and W. Ambach (1988) Solar UVB-albedo of various surfaces. Photochem. Photobiol. 48, 85-88.
- 42. Oke, T. R. (1992) Boundary Layer Climates. Methuen Pub., London, 435 pp.